Beta-Diketone–Cobalt Complexes Sensitize Glioma Stem Cells to Temozolomide Partly Through the ERK-MGMT Pathway

Kaizhi Zhang (zhangkz@jlu.edu.cn)
China-Japan Union Hospital of Jilin University https://orcid.org/0000-0003-2345-2539
Fang Lang
China-Japan Union Hospital of Jilin University
Jing Mang
China-Japan Union Hospital of Jilin University

Research Article

Keywords: Glioblastoma, Cancer stem cell, Combination therapy, Temozolomide, Chemoresistance

Posted Date: August 2nd, 2021

DOI: https://doi.org/10.21203/rs.3.rs-731835/v1

Abstract

Glioblastoma multiforme is characterized by high invasiveness, multidrug resistance, and inevitable recurrence, and current standard treatment regimens are not curative. Even if most glioma cells are eliminated by chemotherapy and radiotherapy, glioma stem cells can survive and differentiate into new tumor cells, thereby triggering tumor recurrence and drug resistance. Therefore, inhibiting tumor invasiveness, reversing drug resistance, and effectively ablating glioma stem cells are critical for improving the prognosis of glioblastoma multiforme. Previous studies reported that the combination of β-diketone–cobalt complexes (CoAc2) and temozolomide (TMZ) has synergistic inhibitory effects on glioma cells. Therefore, we compared cell proliferation, colony-forming capacity, cell migration, and invasion of TMZ-resistant glioma cells and corresponding glioma stem cells after treatment with CoAc2 and/or TMZ. We also explored the underlying mechanism by which CoAc2 sensitizes cells to TMZ through transcriptome sequencing and related signal pathway blockade. We found that CoAc2 significantly increased the inhibitory effect of TMZ on the proliferation, colony formation, migration, invasion, and survival of drug-resistant stem cells. By downregulating ERK pathway activity, CoAc2 inhibited the expression of O6-methylguanine-DNA methyltransferase and eventually sensitized drug-resistant glioma cells to TMZ. In conclusion, the combined use of CoAc2 and TMZ can reverse TMZ resistance and significantly enhance its inhibitory effect on the malignant phenotype of glioma cells and glioma stem cells.

Introduction

As one of the most common primary brain tumors, glioblastoma multiforme (GBM) is highly aggressive and lethal, and it lacks effective treatments because of the particularity of the tissues that it invades[1, 2]. Currently, the main treatment for GBM is surgical resection combined with radiation and cytotoxic chemotherapy[3, 4]. Temozolomide (TMZ) is an alkylating agent that serves as a first-line chemotherapeutic drug for glioma[5].TMZ induces methylation of DNA at the guanine O6 position, leading to double-strand breaks and ultimately cell death[6, 7]. Increasing clinical and basic research data indicate that the abnormal expression of O6-methylguanine-DNA methyltransferase (MGMT) is one of the main causes of TMZ resistance in patients with GBM[8–11]. Therefore, inhibiting MGMT expression can increase the sensitivity of GBM to TMZ and reverse drug resistance[12].

Additionally, GBM is a solid tumor with highly invasiveness because of the proliferation of non-neuronal glial cells, which cannot be completely surgically removed [13, 14]. The heterogeneity of cells in GBM and the subpopulation of self-renewing tumorigenic glioma stem cells (GSCs) induce confer resistance to radiotherapy and chemotherapy, including TMZ[15, 16]. After treatment, surviving GSCs regenerate new tumor cells, leading to GBM recurrence and metastasis [17, 18]. GBM is resistant to conventional treatment, resulting in a poor prognosis. Conventional treatments for GBM only extend the median survival from 12.2 to 14.6 months[19]. To improve patient survival, treatments must be capable of eliminating the entire population of cancer cells, especially GSCs.

Acetylacetone metals contain superoxide anion radicals (O2), which have anti-tumor activity[20]. Cobalt is a trace element required in the human body, and its metal complex has anti-tumor activity[21, 22]. Therefore, we synthesized β-diketone-cobalt complexes [Co(acac)2(H_2O)2, CoAc2]. It has been reported that CoAc2 has cytotoxic effects on liver cancer, ovarian cancer, glioma, and other tumor cells[23, 24]. CoAc2 can inhibit DNA synthesis in tumor cells and induce S-phase arrest. In addition, our previous findings revealed that CoAc2 synergizes the inhibitor effects of TMZ on human glioma cells. Therefore, this study constructed a TMZ-resistant glioma cell line and its corresponding GSCs to verify whether CoAc2 can reverse TMZ resistance, as well as explore the corresponding mechanism.

Materials And Methods

Cell culture

U251 human glioblastoma cells were purchased from China Infrastructure of Cell Line Resource (Beijing, China). Cells were cultured in Dulbecco's modified Eagle's medium (DMEM; Life Tech, USA) supplemented with 10% fetal bovine serum (FBS; BI, Israel) and antibiotics (penicillin and streptomycin, each 100U/mL; Beijing Transgen, China). Cultures were incubated at 37°C in a humidified chamber with 5% CO_2.

For sphere culture in vitro, U251 cells were seeded at 5000 cells/mL in six-well ultralow adherence plates (Corning Inc., USA) in serum-free DMEM/F12 (Life Tech) containing 20 ng/mL recombinant epidermal growth factor (Life Tech), 20 ng/mL basic fibroblast growth factor (Life Tech), B-27™ Supplement (Life Tech), and 1% penicillin/streptomycin (Beijing Transgen). The medium was changed every 48 h.

Cell viability assay

Cells were seeded in 96-well plates at 1 × 10^4 cells per well in 10% FBS-supplemented DMEM. The following day, the cell monolayers were treated with 12.5, 25, 50, 100, 200, or 400 μg/mL TMZ (Aladdin, China) alone or in combination with 1.25, 2.5, 5, 10, or 20 μg/mL CoAc2 (synthesized by our laboratory) for 24 h. MTT solution (5 μg/mL; Sigma, USA) was added (20 μL per well). After 4 h of continuous incubation, the supernatant was discarded, followed by the addition of DMSO (100 μL/well; Solarbio, China). The absorbance at 570 nm was measured. The Chou-Talalay method and CompuSyn software (version 1.0, ComboSyn, Inc., Paramus, USA) were used to detect the interaction between TMZ and CoAc2, which was quantified using a combination index (CI) as follows: CI < 1, synergism; CI = 1, additivity; and CI > 1, antagonism.

After the digestion of spheres in each group, the cells were resuspended in 500 μL of sphere medium, plated into 24-well ultralow adherence plates, and cultured for 4 h with 10 μL of Cell Counting Kit-8 (CCK-8) solution (TransDetect® Cell Counting Kit; Beijing Transgen). Then, 100 μL of culture medium were placed into each well of 96-well plates, and the absorbance at 450 nm was measured using a microplate reader.

Colony formation assays

Glioma cells were seeded into a six-well plate at a density of 1×10^4 cells per well, and the corresponding concentration of drugs was added after 24 h. The medium was changed every 2 days. After 10 days of culture, the cells were fixed with 75% alcohol, stained with crystal violet, dried, and counted.

Immunofluorescent staining

Cells were fixed in 4% paraformaldehyde (PFA) for 30 min, permeabilized in 0.5% Triton X-100 (prepared in PBS) for 20 min at room temperature, and incubated with mouse monoclonal anti-Nestin (1:600; Roche Diagnostics GmbH, Mannheim, Germany) overnight at 4°C. Cells were then incubated for 2 h with goat anti-mouse IgG H&L (Alexa Fluor® 488, 1:400; Abcam, UK), photographed, and observed using a fluorescent microscope.

Protein extraction and Western blot assays

Cells were seeded into a six-well plate and treated with the drugs for 24 h, followed by rinsing with ice-cold PBS solution. The cells were lysed with RIPA lysis buffer (Beyotime, China). The cell supernatant was collected by centrifugation at 12,000 × *g* for 5 min. SDS-PAGE sample loading buffer was added, followed by boiling at 100°C for 5 min. After SDS-PAGE electrophoresis, the total protein was transferred to a PVDF membrane (Millipore, USA), blocked with 5% skim milk for 2 h, and incubated using the primary antibodies overnight at 4°C. After three rinses in TBST, the membrane was incubated with secondary antibodies for 2 h and finally developed using ECL. ImageJ software was used to analyze and quantify protein expression. The primary antibodies included phospho-p44/42 MAPK (Erk1/2) (Thr202/Tyr204) antibody, p44/42 MAPK (Erk1/2) (L34F12) mouse monoclonal antibody (mAb), MGMT (E6M7V) rabbit mAb (CST, USA), and GAPDH (0411) mouse mAb (Santa Cruz, USA). The secondary antibodies were anti-rabbit IgG (HRP-linked) antibody and anti-mouse IgG (HRP-linked) antibody (CST).

Transwell migration and Matrigel® invasion assays

$U251^{TMZ}$ cells were seeded in the upper compartment of 24-well Transwell plates at a density of 3×10^3 cells/well without FBS. For the invasion assay, 100 µL Matrigel® diluted at 1:3 in DMEM was placed in each well of the Transwell and incubated at 37°C for approximately 30 min for solidification before plating transfected cells. The lower compartment was filled with 600 µL DMEM supplemented with 10% FBS. After 48 h of incubation at 37°C in the presence of 5% CO_2, the cells that did not migrate or invade and stayed on the upper surface of the filter were obliterated using a sterile cotton swab. The cells that migrated and invaded through the membrane into the bottom chamber were fixed with 75% ethanol for 30 min and stained with crystal violet. Images captured were used to count cells in randomly selected six fields per well using a microscope (DMI3000B, LEICA). The experiment was repeated three times.

RNA library construction and sequencing

$U251^{TMZ}$ cells were treated with 20 µg/mL CoAc2 or the same volume of DMSO as a control. The total RNA of the cells was extracted using TRIzol after 24 h. The samples were entrusted to GENEWIZ China & Suzhou Lab for subsequent RNA sample quality testing, ribosome removal, library construction, library

purification, library detection, library quantification, and sequencing cluster generation. The samples were finally sequenced and analyzed on the Illumina HiSeq X Ten platform.

Statistical analysis

All experimental data were obtained through three independent experiments and presented as the mean ± SD. Student's *t*-test was used to calculate the statistical significance of the experimental results. $p < 0.05$ denoted statistical significance.

Results

Construction of TMZ-resistant GBM cells

First, we evaluated the cytotoxicity of TMZ in U251 cells. U251 cells were treated with gradient concentrations of TMZ, and the MTT assay was used to detect cell viability. TMZ decreasedthe survival rate of U251 cells in a concentration-dependent manner, and the 50% inhibitory concentration (IC50)was 152.43 ± 15.29 μg/mL (Fig. 1A). TMZ-resistant glioma cells were constructed to explore the mechanism of TMZ resistance in GBM. The initial concentration of TMZ was 1 μg/mL,and it was doubled every 3 weeks. After 21 weeks, $U251^{TMZ}$ cells were harvested as TMZ-resistant cells(Fig. 1B). After 24 h of treatment with 50 μg/mL TMZ, the survival rate of $U251^{TMZ}$cells was 99.89% ± 8.45%, which was significantly higher than that of TMZ-sensitive cells (68.18% ± 3.5%; Fig. 1C). Furthermore, we compared the cytotoxicity of CoAc2 in U251 and $U251^{TMZ}$cells. Although CoAc2 had concentration-dependent cytotoxic activity in both U251 and $U251^{TMZ}$ cells, the cell lines were equally sensitive to the treatment (IC50: 22.01 ± 0.09 μg/mL vs.22.15 ± 2.1 μg/mL).

Effects of TMZ combined with CoAc2 on the proliferation and colony formation of $U251^{TMZ}$cells

Our previous studies indicated that combined treatment with CoAc2 can significantly increase the inhibitory effects of TMZ on glioma cells. Therefore, we further tested whether CoAc2 could reverse TMZ resistance in glioma cells. $U251^{TMZ}$cells were treated with gradient concentrations of CoAc2, TMZ, or both for 24 h, and the survival rate was measured using the MTT assay. Both CoAc2 and TMZ had concentration-dependent effects on $U251^{TMZ}$ cell survival as monotherapy. Combined treatment with > 12.5 μg/mL TMZ and > 2.5 μg/mLCoAc2 had stronger effects on $U251^{TMZ}$cell survival than either therapy alone (Fig. 2A). When the concentrations of TMZ and CoAc2 exceeded 5 and 25 μg/mL, respectively, the CI was less than 1, indicating synergism (Fig. 2A). TMZ (50 μg/mL), CoAc2 (20 μg/mL), or their combination was used to clarify whether CoAc2 could reverse TMZ resistance. After 24 h of treatment, the survival rates of U251 cells treated with TMZ, CoAc2, and both were 59.28% ± 10.63%, 53.57% ± 1.46%, and 30.04% ± 1.01%, respectively, compared with 100% ± 3.82%, 58.06% ± 5.5%, and 24.86% ± 2.99%, respectively, in $U251^{TMZ}$ cells (Fig. 2B). Moreover, the results of the colony formation experiment

illustrated that the combination of TMZ and CoAc2 could significantly inhibit colony formation by $U251^{TMZ}$cells (Fig. 2C).

Effects of TMZ combined with CoAc2 on the migration of $U251^{TMZ}$ cells

We further determine the effect of the combined use of TMZ and CoAc2 on the aggressive behaviors of $U251^{TMZ}$ cells by evaluating migration and invasion. Transwell tumor cell migration and invasion assays illustrated that TMZ had weak inhibitory effects on $U251^{TMZ}$ cell migration and invasion (Fig. 3A, B). Compared with the control group findings, the migration and invasion rates of $U251^{TMZ}$ cells after treatment with TMZ were 90.65% ± 8.92% and 94.47% ± 6.22%, respectively (Fig. 3C, D). Contrarily, CoAc2 strongly inhibited the migration and invasion of $U251^{TMZ}$ cells (Fig. 3A, B). Compared with the control group findings, the migration and invasion rates of $U251^{TMZ}$ cells after treatment with CoAc2 were 65.14% ± 7.19% and 40.46% ± 5.05% (Fig. 3C, D). Compared with the control group data, the migration and invasion rates of $U251^{TMZ}$ cells following treatment with both drugs were 33.54% ± 5.21% and 7.87% ± 3.43%, respectively (Fig. 3C, D).

Reduction of $U251^{TMZ}$ GSCs induced by TMZ and CoAc2

Aggressiveness and high malignancy are highly correlated with GSCs. Therefore, we further tested whether the combination of TMZ and CoAc2 has an inhibitory effect on GSCs. First, $U251^{TMZ}$cells were induced via sphere-formation culture to form spheroid bodies, and immunofluorescence detection revealed that spheroid bodies expressed Nestin, a marker of neural stem cells, indicating that $U251^{TMZ}$ cells were induced to form neurospheres (Fig. 4A). Considering the self-renewal and differentiation capabilities of tumor stem cells, we further tested the passage and differentiation capabilities of the neurospheres. $U251^{TMZ}$ neurospheres cultured in an ultralow attachment plate could be passaged, and the newly formed neurospheres had no obvious morphological changes (Fig. 4B). Subsequently, $U251^{TMZ}$ neurospheres were digested and placed in a serum-containing medium for adherent culture to induce cellular differentiation. These neurospheres could differentiate into mature glioma cells (Fig. 4B). These results indicate that the neurospheres that form after induction of $U251^{TMZ}$ cells have stemness-related properties.

Subsequently, the neurospheres that formed after the 7-day induction of $U251^{TMZ}$ cells were treated with TMZ (50 μg/mL), CoAc2 (20 μg/mL), or both for 2 weeks. The size and number of neurospheres in each group were measured and counted. We then found that TMZ or CoAc2 alone had certain inhibitory effects on the number of neurospheres, and the combination had significantly greater ability to inhibit the number and size of neurospheres than each drug used alone (Fig. 4C, D). Further, the cell counting kit-8 assay revealed that the $U251^{TMZ}$ GSC survival rate after combined treatment with TMZ and CoAc2 was

46.22% ± 3.27%, which was significantly lower than that after TMZ or CoAc2treatment alone (98.35% ± 3.52% and 78.06% ± 5.71%, respectively).

Effect of CoAc2 on gene expression in U251^{TMZ} cells according to RNA-seq

To explore the molecular mechanism by which CoAc2 can reverse TMZ resistance, we performed RNA sequencing in U251TMZ cells treated with CoAc2. First, Gene Ontology (GO) was used to analyze the main biological functions of differential genes of U251^{TMZ} cells after treatment with CoAc2. The enriched GO terms included binding, cell part, and cellular process (Fig. 5A). In addition, Kyoto Encyclopedia of Genes and Genomes functional enrichment analysis was performed on differentially expressed genes. The results identified MAPK signaling pathway genes as the most significant differentially expressed genes, and the enrichment degree was relatively large (Fig. 5B). Furthermore, differentially expressed proteins in U251^{TMZ}cellswere detected after treatment with TMZ (50 μg/mL), CoAc2 (20 μg/mL), or both. We found that TMZ alone had no effect on MGMT expression, whereas CoAc2 alone significantly downregulated phospho-Erk1/2 and MGMT expression. Both phospho-Erk1/2 and MGMT were significantly downregulated after combined treatment with TMZ and CoAc2.

Inhibitory effects of TMZ combined with mitogen-activated protein kinase (MEK) inhibitors on TMZ-resistant glioma cells

To verify the role of the ERK pathway in TMZ resistance, we tested the effects of the MEK inhibitorPD98059 (25 μM) and TMZ (50 μg/mL) on drug-resistant cells. The addition of CoAc2 or PD98059 to TMZ resulted in significant downregulation of phospho-Erk1/2 and MGMT (Fig. 6A). The migration and invasion rates of U251^{TMZ} cells after combined treatment with PD98059 and TMZ were 48.14% ± 2.90% and 18.38% ± 2.24%, respectively, compared with 36.69% ± 3.99% and 10.98% ± 2.45%, respectively, after treatment with CoAc2 and TMZ (Fig. 6B–E).

Subsequently, the neurospheres that formed after 7-day induction of U251^{TMZ} cells were treated with TMZ (50 μg/mL) combined with PD98059 (25 μM) or CoAc2 (20 μg/mL) for 2 weeks. The size and number of neurospheres in each group were measured and counted. We found that both combinations had significant inhibitory effects on the number and size of neurospheres (Fig. 7A, B). CCK-8 analysis of the cells revealed that the survival rates of U251^{TMZ} GSCs after PD98059/TMZ and CoAc2/TMZ treatment were 56.72% ± 4.35% and 46.55% ± 2.96%, respectively (Fig. 7C).

Discussion

GBM is the most common and aggressive tumor of the central nervous system,and it carries the worst prognosis [25]. TMZ is a first-line chemotherapy for glioma, but most patients with glioma will develop resistance [26]. Studies have revealed that CDC2 expression is negatively correlated with the TMZ

sensitivity of gliomas. High CDC2 expression in patients with glioma portends a poor prognosis and short overall survival[27]. In addition, LncRNA-XIST reduces the sensitivity of gliomas to TMZ by inhibiting miR-29c and upregulating SP1 and MGMT. Patients with high LncRNA-XIST expression have short overall survival[28]. Therefore, increasing the sensitivity of glioma to TMZ may be an effective strategy to improve the overall survival of patients.

Moreover, the mechanism by which the sensitivity of glioma to TMZ is enhanced can also be used to reverse TMZ resistance in this malignancy. Our previous study found that CoAc2 can increase the sensitivity of human glioma cells to TMZ, and moreover, there is a synergistic effect between CoAc2 and TMZ. Therefore, we attempted to verify whether CoAc2 can reverse TMZ resistance in glioma. In this study, we used the method of concentration doubling to generate the TMZ-resistant cell line $U251^{TMZ}$ and confirmed that these cells were resistant to TMZ but not CoAc2. Further examination demonstrated that CoAc2 both reversed resistance to TMZ and synergized its cytotoxic effects in both TMZ-sensitive and TMZ-resistant glioma cells.

GBM cannot be completely removed via surgical resection because of its high invasiveness; it is also prone to develop resistance to chemotherapy because of tumor heterogeneity and tumor stem cells [29]. Extensive evidence indicates that tumor stem cells are related to chemotherapy resistance and tumor maintenance and recurrence; therefore, we further demonstrated that the combined use of TMZ and CoAc2 significantly inhibited the proliferation of GSCs. In addition, the combination regimen significantly inhibited colony formation, migration, and invasion by $U251^{TMZ}$ cells.

In this study, RNA-seq was performed on $U251^{TMZ}$ cells treated with CoAc2. Based on previous findings, we focused on the ERK pathway and found that CoAc2 decreased Erk1/2 phosphorylation and inhibited the expression of the TMZ resistance gene MGMT. Some studies have reported that MEK inhibition activates p53 that downregulates MGMT expression [30–32]. The methyl group of the O6 position of guanine added by TMZ is removed by MGMT, which prevents cell death by mismatch repair (MMR) [9, 33, 34]. Elevating ERK activation increases protein levels of stemness markers in GSC, and inhibiting ERK activation impairs sphere formation and attenuates the expression of genes associated with neural cancer stemness[35, 36]. Our results suggested that CoAc2 might reverse TMZ resistance by inhibiting the activation of the ERK pathway. Thus, we used the MEK inhibitor PD98059 [37] in combination with TMZ and found that inhibiting ERK pathway activation could downregulate the expression of MGMT. This regimen also inhibited the migration and invasion of $U251^{TMZ}$ cells similarly as TMZ plus CoAc2. However, the finding that the combination of CoAc2 and TMZ more strongly inhibited the proliferation of GSCs than TMZ plus PD98059 indicated that CoAc2 reverses TMZ resistance through multiple effects including inhibition of the ERK pathway.

In conclusion, the present study highlights the importance of CoAc2 in the sensitization of GSCs to TMZ, mediated partially via the ERK-MGMT pathway.

Declarations

Acknowledgments

The authors would like to thank Lab Center, China-Japan Union Hospital of Jilin University, China for providing laboratory equipment.

Author contributions

Kaizhi Zhang: Cell culture, proliferation, migration and invasion assays. Fang Lang: Protein extraction, western blot assays, and immunofluorescent staining. Jing Mang: Statistical analysis and writing.

Funding

This work was supported by the National Natural Science Foundation of China (81672492)Jilin Province Department of Finance (SCZSY201724) and Jilin Province Development and Reform Commission (2015Y030-7). The funders had no role in study design, data collection and analysis, decision to publish, or preparation of the manuscript.

Data availability

Data archiving is not mandated but data will be made available on reasonable request.

Compliance with ethical standards

Conflict of interest

These authors declare that they have no conflicts of interests.

Ethics approval

The study includes only laboratory studies on a stable established cell line. No ethical or institutional approval was required.

References

1. Batash R, Asna N, Schaffer P, Francis N, Schaffer M (2017) Glioblastoma Multiforme, Diagnosis and Treatment; Recent Literature Review. Curr Med Chem 24:3002–3009. doi:10.2174/0929867324666170516123206
2. Le Rhun E, Preusser M, Roth P, Reardon DA, van den Bent M, Wen P, Reifenberger G, Weller M (2019) Molecular targeted therapy of glioblastoma. Cancer Treat Rev 80:101896. doi:10.1016/j.ctrv.2019.101896
3. Alifieris C, Trafalis DT (2015) Glioblastoma multiforme: Pathogenesis and treatment. Pharmacol Ther 152:63–82. doi:10.1016/j.pharmthera.2015.05.005
4. Campos B, Olsen LR, Urup T, Poulsen HS (2016) A comprehensive profile of recurrent glioblastoma. Oncogene 35:5819–5825. doi:10.1038/onc.2016.85

5. Gerstner ER, Emblem KE, Chang K, Vakulenko-Lagun B, Yen YF, Beers AL, Dietrich J, Plotkin SR, Catana C, Hooker JM, Duda DG, Rosen B, Kalpathy-Cramer J, Jain RK, Batchelor T (2020) Bevacizumab Reduces Permeability and Concurrent Temozolomide Delivery in a Subset of Patients with Recurrent Glioblastoma. Clin Cancer Res 26:206–212. doi:10.1158/1078-0432.Ccr-19-1739
6. Tomar VS, Patil V, Somasundaram K (2020) Temozolomide induces activation of Wnt/β-catenin signaling in glioma cells via PI3K/Akt pathway: implications in glioma therapy. Cell Biol Toxicol 36:273–278. doi:10.1007/s10565-019-09502-7
7. Chen WJ, Zhang X, Han H, Lv JN, Kang EM, Zhang YL, Liu WP, He XS, Wang J, Wang GH, Yu YB, Zhang W (2020) The different role of YKL-40 in glioblastoma is a function of MGMT promoter methylation status. Cell Death Dis 11:668. doi:10.1038/s41419-020-02909-9
8. Lee SY (2016) Temozolomide resistance in glioblastoma multiforme. Genes Dis 3:198–210. doi:10.1016/j.gendis.2016.04.007
9. Chen X, Zhang M, Gan H, Wang H, Lee JH, Fang D, Kitange GJ, He L, Hu Z, Parney IF, Meyer FB, Giannini C, Sarkaria JN, Zhang Z (2018) A novel enhancer regulates MGMT expression and promotes temozolomide resistance in glioblastoma. Nat Commun 9:2949. doi:10.1038/s41467-018-05373-4
10. Stupp R, Hegi ME, Gorlia T, Erridge SC, Perry J, Hong YK, Aldape KD, Lhermitte B, Pietsch T, Grujicic D, Steinbach JP, Wick W, Tarnawski R, Nam DH, Hau P, Weyerbrock A, Taphoorn MJ, Shen CC, Rao N, Thurzo L, Herrlinger U, Gupta T, Kortmann RD, Adamska K, McBain C, Brandes AA, Tonn JC, Schnell O, Wiegel T, Kim CY, Nabors LB, Reardon DA, van den Bent MJ, Hicking C, Markivskyy A, Picard M, Weller M (2014) Cilengitide combined with standard treatment for patients with newly diagnosed glioblastoma with methylated MGMT promoter (CENTRIC EORTC 26071 – 22072 study): a multicentre, randomised, open-label, phase 3 trial. Lancet Oncol 15:1100–1108. doi:10.1016/s1470-2045(14)70379-1
11. Cros J, Hentic O, Rebours V, Zappa M, Gille N, Theou-Anton N, Vernerey D, Maire F, Levy P, Bedossa P, Paradis V, Hammel P, Ruszniewski P, Couvelard A (2016) MGMT expression predicts response to temozolomide in pancreatic neuroendocrine tumors. Endocr Relat Cancer 23:625–633. doi:10.1530/ERC-16-0117
12. Taylor JW, Schiff D (2015) Treatment considerations for MGMT-unmethylated glioblastoma. Curr Neurol Neurosci Rep 15:507. doi:10.1007/s11910-014-0507-z
13. Grek CL, Sheng Z, Naus CC, Sin WC, Gourdie RG, Ghatnekar GG (2018) Novel approach to temozolomide resistance in malignant glioma: connexin43-directed therapeutics. Curr Opin Pharmacol 41:79–88. doi:10.1016/j.coph.2018.05.002
14. Drean A, Goldwirt L, Verreault M, Canney M, Schmitt C, Guehennec J, Delattre JY, Carpentier A, Idbaih A (2016) Blood-brain barrier, cytotoxic chemotherapies and glioblastoma. Expert Rev Neurother 16:1285–1300. doi:10.1080/14737175.2016.1202761
15. Bao S, Wu Q, McLendon RE, Hao Y, Shi Q, Hjelmeland AB, Dewhirst MW, Bigner DD, Rich JN (2006) Glioma stem cells promote radioresistance by preferential activation of the DNA damage response. Nature 444:756–760. doi:10.1038/nature05236

16. Gimple RC, Bhargava S, Dixit D, Rich JN (2019) Glioblastoma stem cells: lessons from the tumor hierarchy in a lethal cancer. Genes Dev 33:591–609. doi:10.1101/gad.324301.119
17. Jhaveri N, Chen TC, Hofman FM (2016) Tumor vasculature and glioma stem cells: Contributions to glioma progression. Cancer Lett 380:545–551. doi:10.1016/j.canlet.2014.12.028
18. Lamszus K, Günther HS (2010) Glioma stem cells as a target for treatment. Target Oncol 5:211–215. doi:10.1007/s11523-010-0155-4
19. Tabatabai G, Weller M (2011) Glioblastoma stem cells. Cell Tissue Res 343:459–465. doi:10.1007/s00441-010-1123-0
20. Patra D, Paul S, Majumder I, Sepay N, Bera S, Kundu R, Drew MGB, Ghosh T (2017) Exploring the effect of substituent in the hydrazone ligand of a family of mu-oxidodivanadium(v) hydrazone complexes on structure, DNA binding and anticancer activity. Dalton Trans 46:16276–16293. doi:10.1039/c7dt03585c
21. Kelland L (2007) The resurgence of platinum-based cancer chemotherapy. Nat Rev Cancer 7:573–584. doi:10.1038/nrc2167
22. Mohapatra SR, Sadik A, Tykocinski LO, Dietze J, Poschet G, Heiland I, Opitz CA (2019) Hypoxia Inducible Factor 1alpha Inhibits the Expression of Immunosuppressive Tryptophan-2,3-Dioxygenase in Glioblastoma. Front Immunol 10:2762. doi:10.3389/fimmu.2019.02762
23. Zhang K, Zhao X, Liu J, Fang X, Wang X, Wang X, Li R (2014) β-diketone-cobalt complexes inhibit DNA synthesis and induce S-phase arrest in rat C6 glioma cells. Oncol Lett 7:881–885. doi:10.3892/ol.2013.1772
24. Zhang K, Cui S, Wang J, Wang X, Li R (2012) Study on antitumor activity of metal-based diketone complexes. Med Chem Res 21:1071–1076. doi:10.1007/s00044-011-9618-0
25. Rosenfeld MR, Ye X, Supko JG, Desideri S, Grossman SA, Brem S, Mikkelson T, Wang D, Chang YC, Hu J, McAfee Q, Fisher J, Troxel AB, Piao S, Heitjan DF, Tan KS, Pontiggia L, O'Dwyer PJ, Davis LE, Amaravadi RK (2014) A phase I/II trial of hydroxychloroquine in conjunction with radiation therapy and concurrent and adjuvant temozolomide in patients with newly diagnosed glioblastoma multiforme. Autophagy 10:1359–1368. doi:10.4161/auto.28984
26. Chinot OL, Wick W, Mason W, Henriksson R, Saran F, Nishikawa R, Carpentier AF, Hoang-Xuan K, Kavan P, Cernea D, Brandes AA, Hilton M, Abrey L, Cloughesy T (2014) Bevacizumab plus radiotherapy-temozolomide for newly diagnosed glioblastoma. N Engl J Med 370:709–722. doi:10.1056/NEJMoa1308345
27. Zhou B, Bu G, Zhou Y, Zhao Y, Li W, Li M (2015) Knockdown of CDC2 expression inhibits proliferation, enhances apoptosis, and increases chemosensitivity to temozolomide in glioblastoma cells. Med Oncol 32:378. doi:10.1007/s12032-014-0378-9
28. Du P, Zhao H, Peng R, Liu Q, Yuan J, Peng G, Liao Y (2017) LncRNA-XIST interacts with miR-29c to modulate the chemoresistance of glioma cell to TMZ through DNA mismatch repair pathway. Biosci Rep 37. doi:10.1042/bsr20170696

29. Lathia JD, Mack SC, Mulkearns-Hubert EE, Valentim CL, Rich JN (2015) Cancer stem cells in glioblastoma. Genes Dev 29:1203–1217. doi:10.1101/gad.261982.115
30. Sato A, Sunayama J, Matsuda K, Seino S, Suzuki K, Watanabe E, Tachibana K, Tomiyama A, Kayama T, Kitanaka C (2011) MEK-ERK signaling dictates DNA-repair gene MGMT expression and temozolomide resistance of stem-like glioblastoma cells via the MDM2-p53 axis. Stem Cells 29:1942–1951. doi:10.1002/stem.753
31. Li Q, Ren B, Gui Q, Zhao J, Wu M, Shen M, Li D, Li D, Chen K, Tao M, Liang R (2020) Blocking MAPK/ERK pathway sensitizes hepatocellular carcinoma cells to temozolomide via downregulating MGMT expression. Ann Transl Med 8:1305. doi:10.21037/atm-20-5478
32. Jiapaer S, Furuta T, Dong Y, Kitabayashi T, Sabit H, Zhang J, Zhang G, Tanaka S, Kobayashi M, Hirao A, Nakada M (2020) Identification of 2-Fluoropalmitic Acid as a Potential Therapeutic Agent Against Glioblastoma. Curr Pharm Des 26:4675–4684. doi:10.2174/1381612826666200429092742
33. Butler M, Pongor L, Su Y-T, Xi L, Raffeld M, Quezado M, Trepel J, Aldape K, Pommier Y, Wu J (2020) MGMT Status as a Clinical Biomarker in Glioblastoma. Trends in cancer 6:380–391. doi:10.1016/j.trecan.2020.02.010
34. Ni XR, Guo CC, Yu YJ, Yu ZH, Cai HP, Wu WC, Ma JX, Chen FR, Wang J, Chen ZP (2020) Combination of levetiracetam and IFN-alpha increased temozolomide efficacy in MGMT-positive glioma. Cancer Chemother Pharmacol 86:773–782. doi:10.1007/s00280-020-04169-y
35. Kwon SJ, Kwon OS, Kim KT, Go YH, Yu SI, Lee BH, Miyoshi H, Oh E, Cho SJ, Cha HJ (2017) Role of MEK partner-1 in cancer stemness through MEK/ERK pathway in cancerous neural stem cells, expressing EGFRviii. Mol Cancer 16:140. doi:10.1186/s12943-017-0703-y
36. Yu Y, Chen C, Huo G, Deng J, Zhao H, Xu R, Jiang L, Chen S, Wang S (2019) ATP1A1 Integrates AKT and ERK Signaling via Potential Interaction With Src to Promote Growth and Survival in Glioma Stem Cells. Front Oncol 9:320. doi:10.3389/fonc.2019.00320
37. Eluka-Okoludoh E, Ewunkem AJ, Thorpe S, Blanchard A, Muganda P (2018) Diepoxybutane-induced apoptosis is mediated through the ERK1/2 pathway. Hum Exp Toxicol 37:1080–1091. doi:10.1177/0960327118755255

Figures

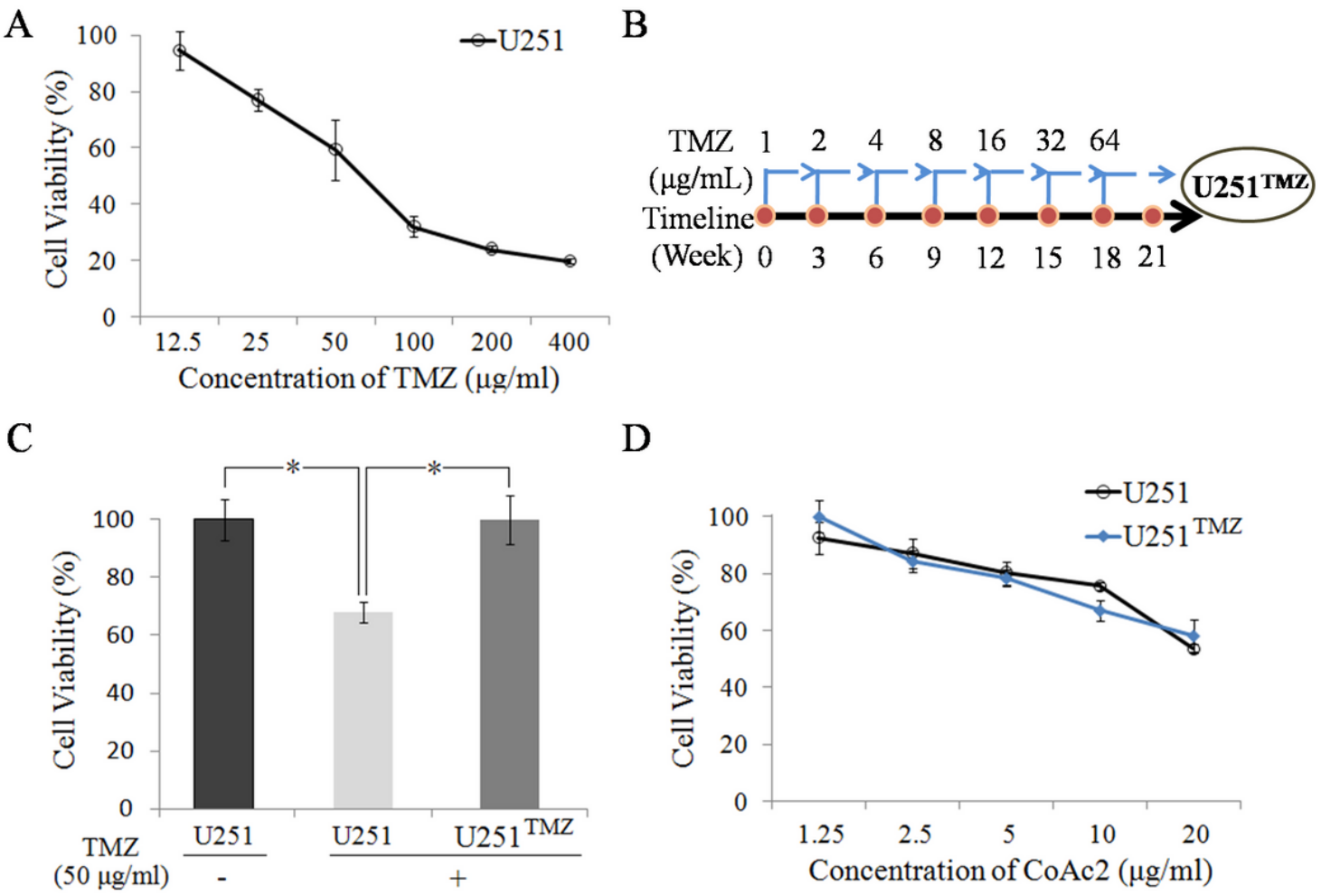

Figure 1

Construction of TMZ-resistant U251 cells (U251TMZ cells). (A) U251 cells were plated onto 96-well plates and treated with different concentrations of CoAc2 (1.25–400 μg/mL) for 24 h, followed by assessments of cell growth using the MTT assay. (B) Timeline chart of TMZ resistance in U251 cells. (C) After 24 h of treatment with TMZ (50 μg/mL), the cell survival ratein U251 and U251TMZcells was measured using the MTT assay. *p< 0.05. (D) U251 and U251TMZ cells were plated onto 96-well plates and treated with different concentrations of CoAc2 (1.25–20 μg/mL) for 24 h, followed by assessments of cell growth using the MTT assay. TMZ:temozolomide; CoAc2: β-diketone-cobalt complexes.

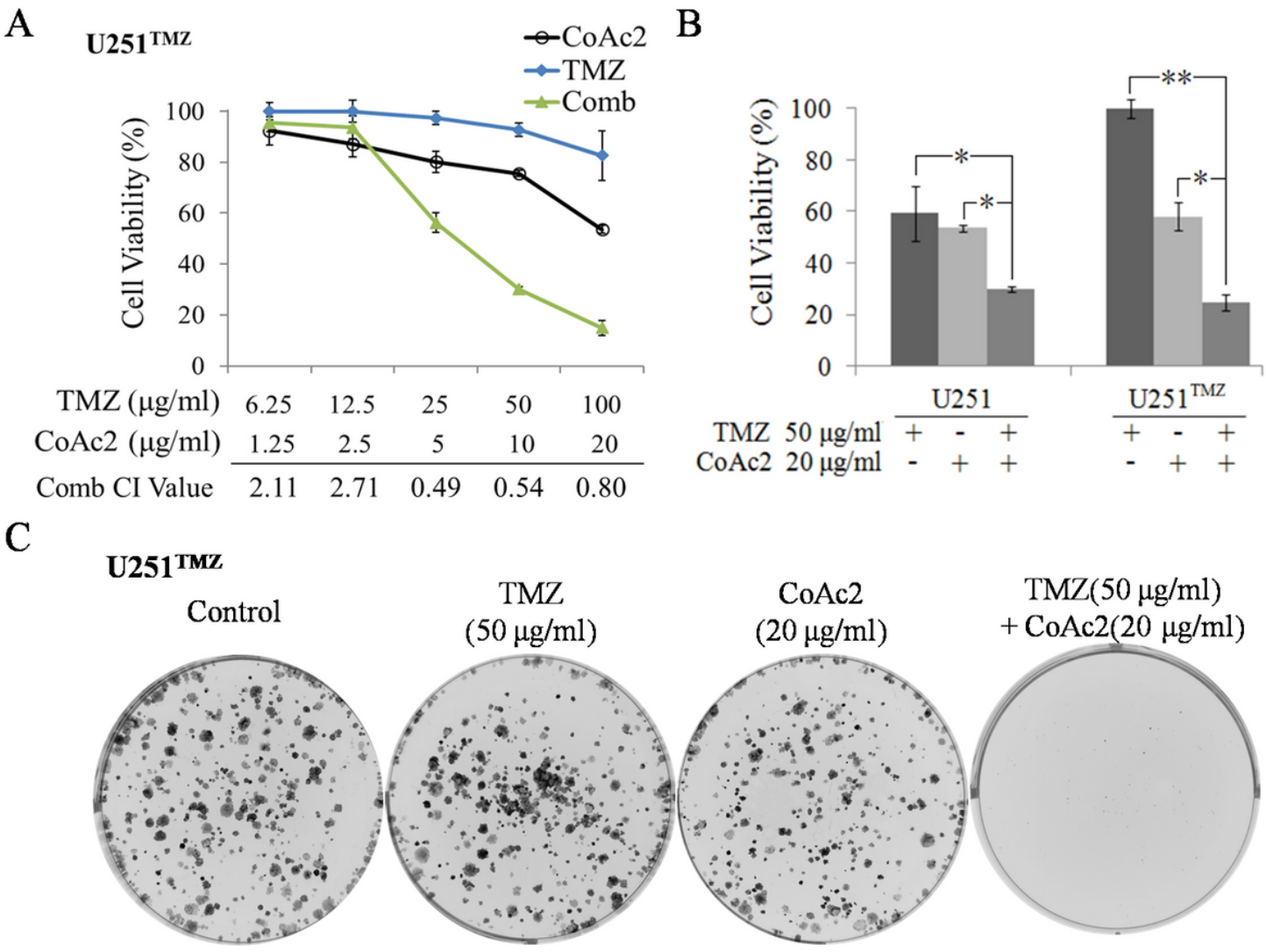

Figure 2

CoAc2 enhanced the TMZ-induced inhibition of cell proliferation and clone formation in U251TMZ cells. (A) U251TMZ cells were plated onto 96-well plates and treated with different concentrations of CoAc2 (1.25–20 μg/mL), TMZ (6.25–100 μg/mL), or both for 24 h, followed by assessments of cell growth using the MTT assay. The combination index (CI) was calculated for the CoAc2 and TMZ concentrations used in the MTT assays. (B) After 24 h of treatment with TMZ (50 μg/mL), CoAc2 (20 μg/mL), or both (Comb), the cell survival rate of U251 and U251TMZ cells was measured using the MTT assay. *p< 0.05; **p< 0.01. (C) After 24 h of culture of U251TMZ cells in six-well plates (1 × 103 cells per well), the cells were treated with TMZ (50 μg/mL), CoAc2 (20 μg/mL), or both (Comb) for 1 week, to detect colony formation. TMZ:temozolomide; CoAc2: β-diketone-cobalt complexes.

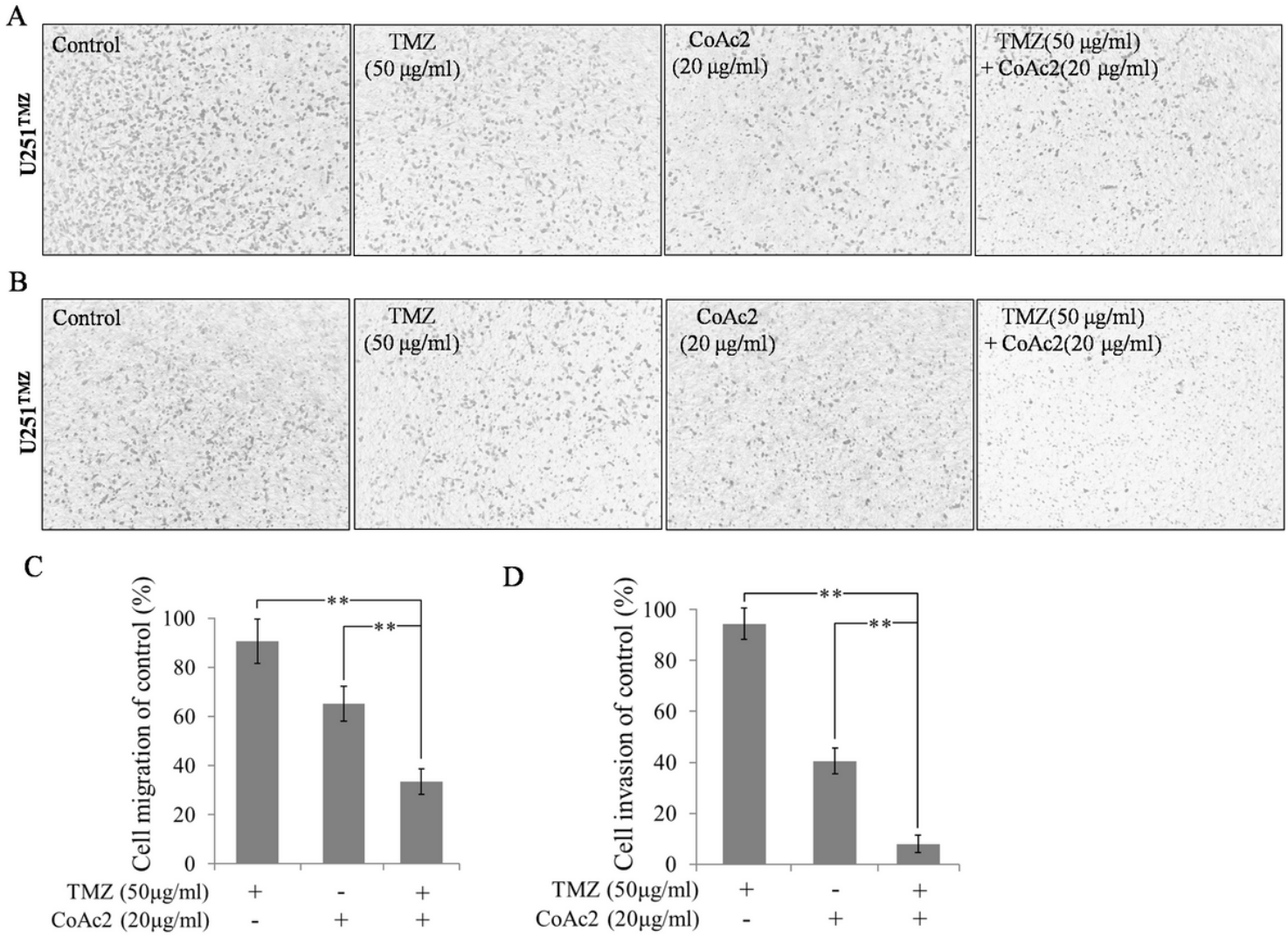

Figure 3

CoAc2 combined with TMZ significantly inhibits the migration of U251TMZcells. (A) U251TMZ cells were plated into Transwell chambers. After 48 h of culture with CoAc2 (20 μg/mL), TMZ (50 μg/mL), or both, and cell migration was detected using the Transwell migration assay and presented relative to the control (C). ** p< 0.01. (B) U251TMZ cells were plated into the Matrigel-covered Transwell chamber.After 48 h of culture with CoAc2 (20 μg/mL), TMZ (50 μg/mL), or both, cell invasion was detected using Transwell invasion assay and presented relative to the control (D). **p< 0.01. TMZ:temozolomide; CoAc2: β-diketone-cobalt complexes.

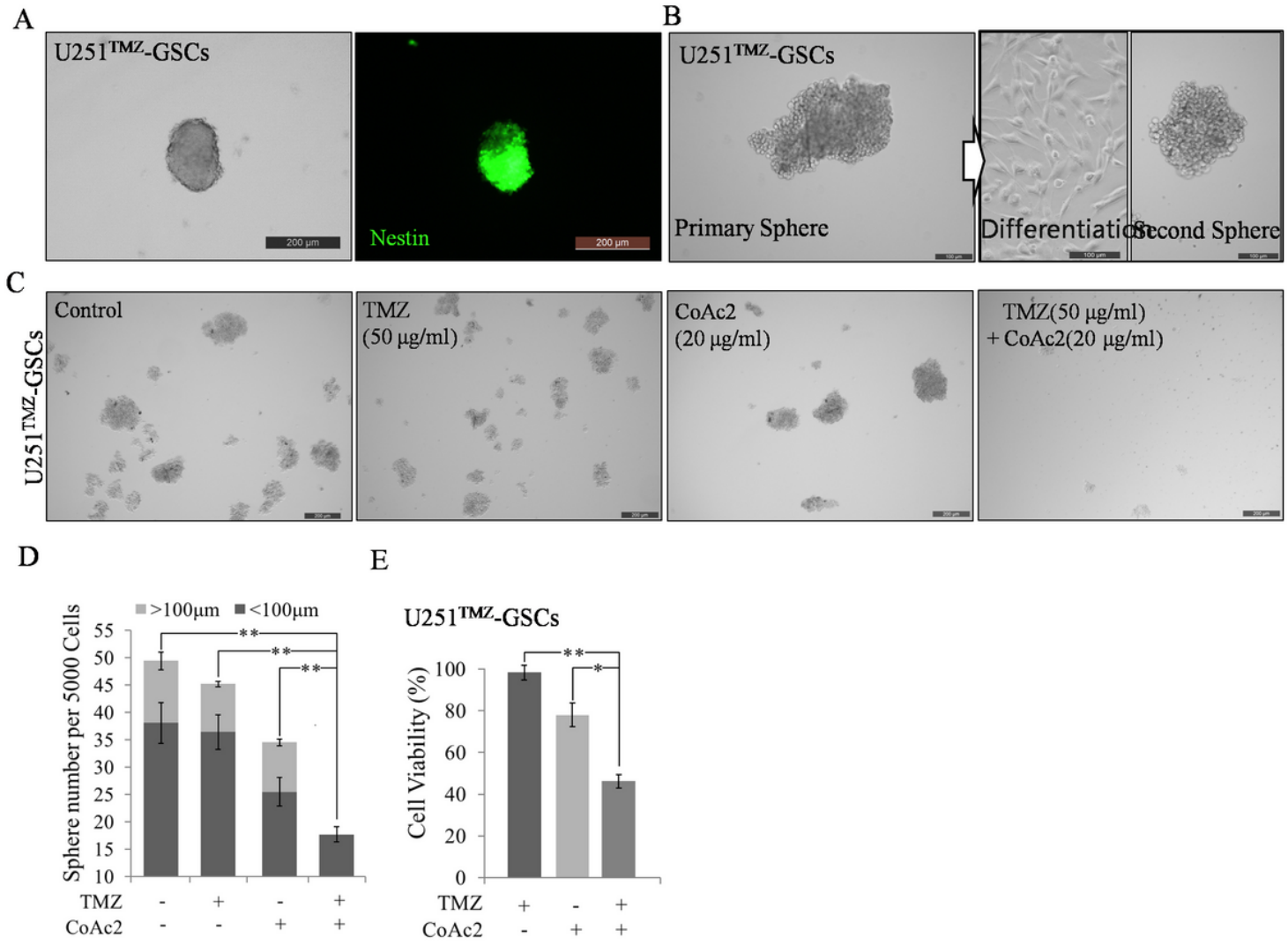

Figure 4

CoAc2 combined with TMZ significantly inhibits the proliferation of U251TMZ GSCs. (A) U251TMZ cells were seeded at 5000 cells/mL in six-well ultralow adherence plates in CSC medium for 7 days to permit neurosphere formation. Immunofluorescence-labeled neural surface marker Nestin (Green). Scale bar = 200 μm. (B) The neurospheres formed in serum-free suspension cultures of U251TMZcells could be continuously passaged without significant changes in morphology. In addition, neurospheres were reattached to plates to induce cellular differentiation. Scale bar = 200 μm. (C) U251TMZ cells (5000 cells/mL) were cultured in CSC medium for 7 days to form neurospheres that were then treated with CoAc2 (20 μg/mL), TMZ (50 μg/mL), or both for 2 weeks. Neurosphere formation was determined via microscopic examination. Scale bar = 200 μm. (D) The neurospheres were quantitated. **p< 0.01. (E) The neurospheres were separated and seeded into 96-well plates, and Cell Counting Kit-8 was used to detect cell viability. * p < 0.05; ** p < 0.01. TMZ:temozolomide; CoAc2: β-diketone-cobalt complexes; GSC, glioma stem cell.

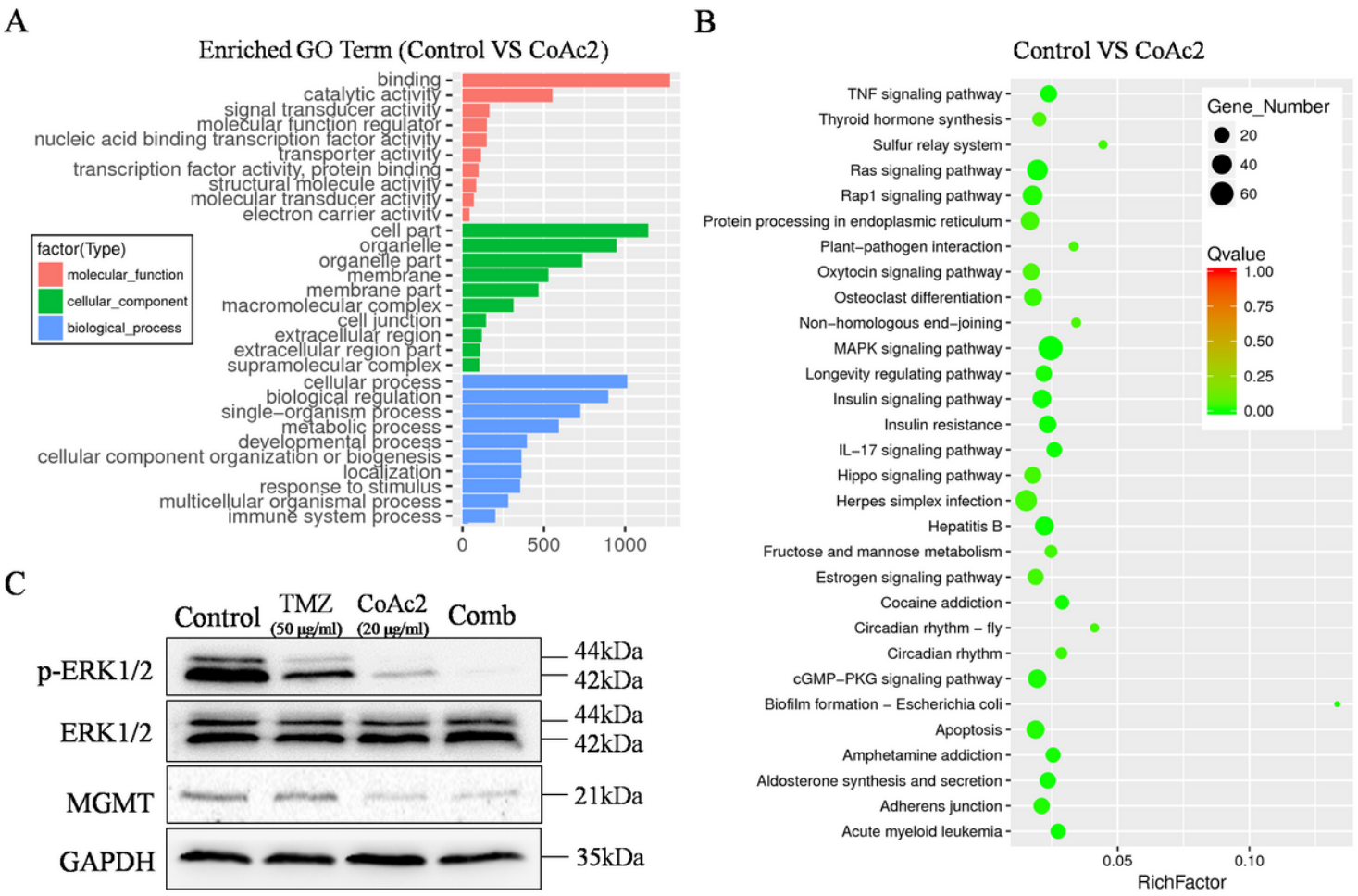

Figure 5

Expression profile analysis of CoAc2-treated U251TMZ cells via RNA-seq and bioinformatics. (A) Gene Ontology (GO) enrichment analysis and (B) scatter plot of candidate target genes enriched in the pathways. U251TMZcells were treated with CoAc2 (20 μg/mL) for 24 h, followed by transcriptome sequencing analysis. Richfactor refers to the ratio of the number of differentially expressed genes to the total number of annotated genes located in the pathway entry. A higher Richfactor indicates a higher degree of enrichment. Qvalue is the p-value after multiple hypothesis testing and correction. The range of Qvalue is [0, 1], with values closer to zero indicating greater enrichment. (C) Western blot analysis of protein expression changes in U251TMZcells after treatment with CoAc2 (20 μg/mL), TMZ (50 μg/mL), or both. TMZ:temozolomide; CoAc2: β-diketone-cobalt complexes; MGMT, O6-methylguanine-DNA methyltransferase.

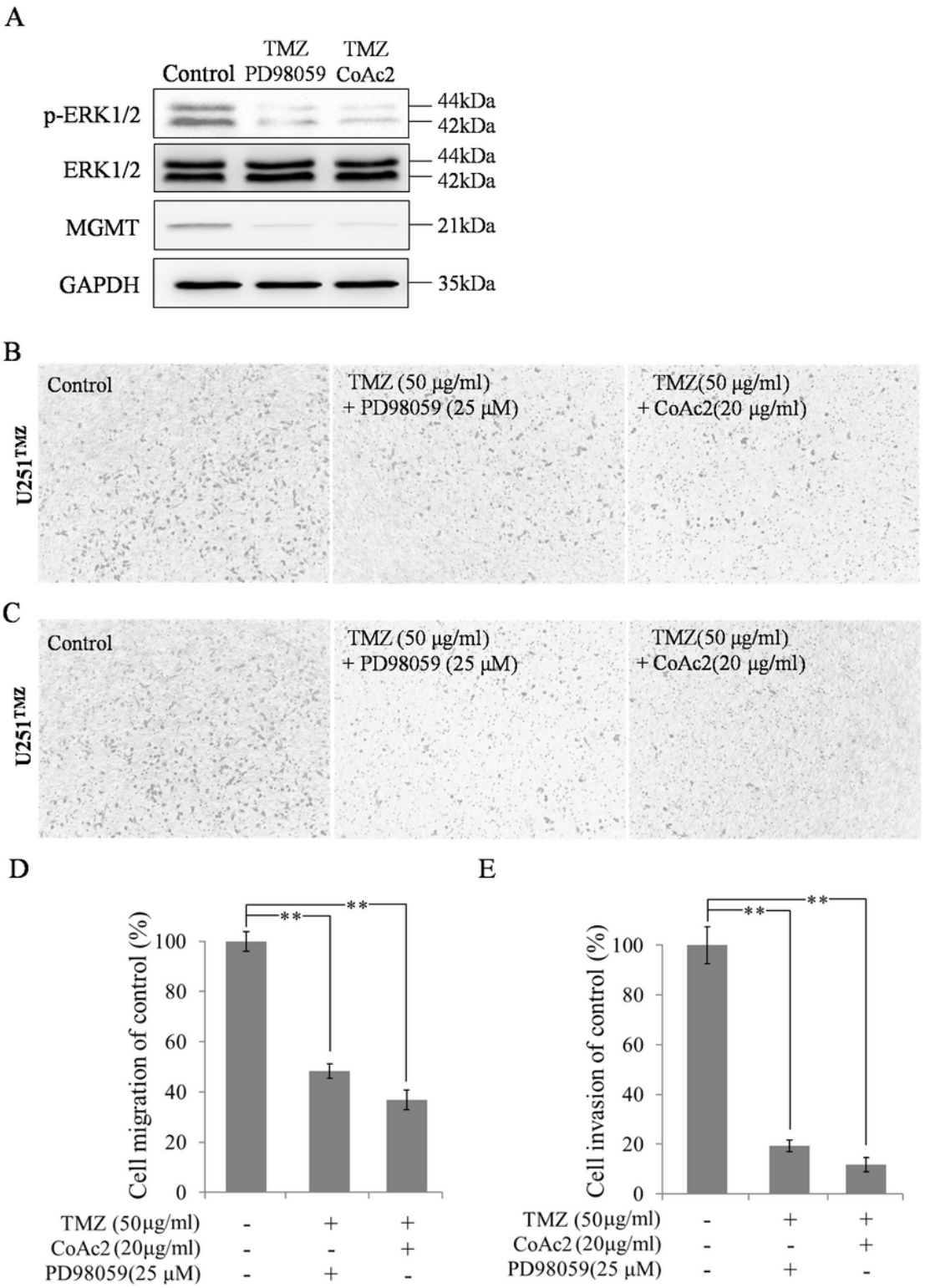

Figure 6

PD98059 combined with TMZ significantly inhibits the migration of U251TMZ cells. (A) Western blotting was used to analyze protein expression in U251TMZ cells after treatment with TMZ (50 μg/mL) combined with PD98059 (25 μM) or CoAc2 (20 μg/mL). (B) U251TMZcells were plated into the Transwell chamber and cultured with TMZ (50 μg/mL) combined with PD98059 (25 μM) or CoAc2 (20 μg/mL) for 48 h. Cell migration was detected using the Transwell migration assay with relative quantification (D). **

p < 0.01. (C) U251TMZ cells were plated into the Matrigel-covered Transwell chamber and cultured with TMZ (50 μg/mL) combined with PD98059 (25 μM) or CoAc2 (20 μg/mL) for 48 h. Cell migration was detected using Transwell migration assay with relative quantification (E). ** p < 0.01. TMZ:temozolomide; CoAc2: β-diketone-cobalt complexes.

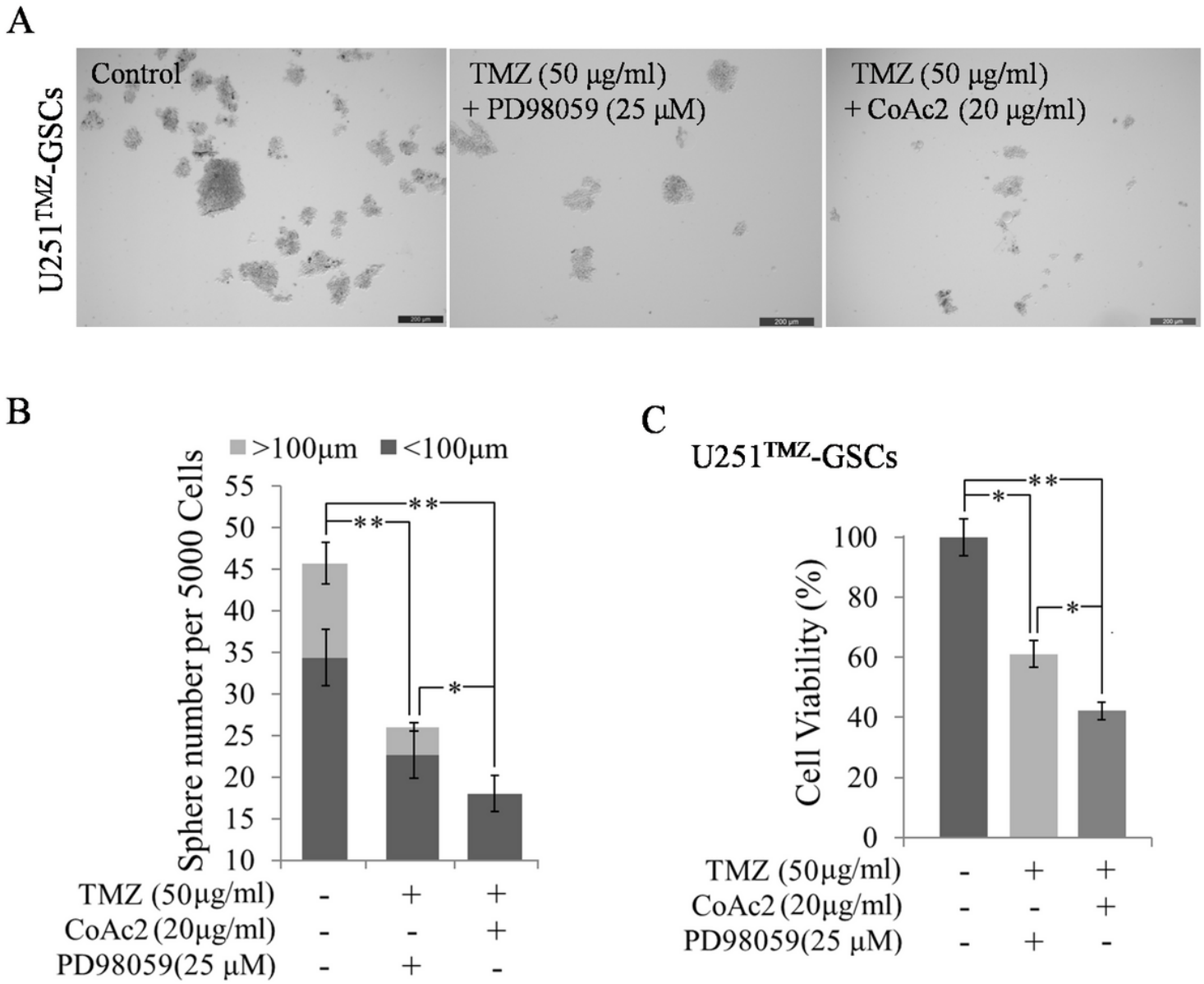

Figure 7

PD98059 combined with TMZ significantly inhibits the proliferation of U251TMZ GSCs. (C) U251TMZ cells (5000 cells/mL) were cultured in CSC medium for 7 days to permit neurosphere formation. Neurospheres werethen cultured with PD98059 (25 μM), CoAc2 (20 μg/mL), and TMZ (50 μg/mL) after 2 weeks. Neurosphere formation was determined via microscopic examination. Scale bar = 200 μm. (D) The neurospheres were quantitated. **p < 0.01. (E) The neurospheres were separated and seeded into 96-well plates, and Cell Counting Kit-8 was used to detect cell viability. * p < 0.05; ** p < 0.01. TMZ:temozolomide; CoAc2: β-diketone-cobalt complexes; GSC, glioma stem cell.